ISSN 2070-2051, Protection of Metals and Physical Chemistry of Surfaces, 2015, Vol. 51, No. 4, pp. 693–700. © Pleiades Publishing, Ltd., 2015.

PHYSICOCHEMICAL PROBLEMS OF MATERIALS PROTECTION

Pitting Corrosion Inhibition of Type 304 Austenitic Stainless steel by 2-Amino-5-ethyl-1,3,4-thiadiazole in Dilute Sulphuric Acid

R. T. Loto[a,b] and C. A. Loto[a,b]

[a] *Department of Mechanical Engineering, Covenant University, Ota, Ogun State, Nigeria*

[b] *Department of Chemical, Metallurgical and Materials Engineering, Tshwane University of Technology, Pretoria, South Africa*

e-mail: tolu.loto@gmail.com

Received March 20, 2014

Abstract—The electrochemical behaviour and inhibitor protection of 2-amino-5-ethyl-1,3,4-thiadiazole (TTD) on the pitting corrosion of austenitic stainless steel (type 304) in dilute sulphuric acid solution contaminated with recrystallised sodium chloride was evaluated with the aid of potentiodynamic polarization method. TTD greatly reduced the corrosion rate of the steel with a corrosion inhibition efficiency ranging from 88.99–87.36%. The corrosion potential, pitting potential, repassivation potential, nucleation resistance, passivation range and repassivation capacity measurements and potentiodynamic studies were applied to assess the steel's pitting resistance characteristics and behaviour in the acid chloride media. Results showed that pitting potential values increased with addition of TTD compound in conjunction with increase in the passivation range which strongly indicating increased electrochemical resistance to pitting corrosion.

DOI: 10.1134/S2070205115040231

INTRODUCTION

Corrosion induced damage on metallic alloy and stainless steels are a major problem to industrial production and operating facilities and equipments due to metal degradation and insidious attacks such as pitting corrosion. These results in production loss, costly maintenance and high operating cost. In addition, leaks of process fluids may also lead to unacceptable health and safety hazards, risk of damage to the environment, as well as the associated clean-up costs. All of these expenditures can have a huge financial impact to the operating company. The corrosion resistance of stainless steel is due to the formation of a strong adherent, compact and continuous oxide film of chromium on the steel surface. In aqueous acid solutions the passive film is basically of duplex nature, consisting of a chromium-rich inner barrier oxide layer and iron-rich outer deposited hydroxide or salt layer [1–10]. The passive films are vulnerable to localized attack especially at regions of flaws or defects by corrosive ions such as chlorides, sulphates, thiosulphates, bromides etc eventually leading to pitting corrosion and intensive structural damage.

Breakdown of the passive film from pit initiation occurs at a critical potential called pitting potential, E_{pit}. This is one of the important parameters that typify the susceptibility of stainless steel to pitting corrosion. Significant number of attempts has been done to investigate the pitting of stainless steel [11], however most of the theoretical assumptions suggests that chloride ions diffuses through the passive films before film breakdown upon reaching the metal/film interface. The pitting processes can be divided into two, the first passive film breakdown and the consequent metal substrate dissolution. Generally pitting corrosion is invariably the most destructive form of corrosion especially due to difficulty in predicting its occurrence. As complexity of the corrosive environment increases, the accuracy of the determinant parameters for pitting corrosion evaluation decreases. The corrosion process occurs in a series of steps beginning with the initiation stage which itself is a product of various phenomena that are mainly properties of the solution and those of the metal [12–17].

Aqueous sulphuric acid solutions containing chlorides have been employed in the investigation of the passivation behaviour of stainless steel [18–21], due to the combined action of the aggressive ions and high reproducibility of the pitting corrosion parameter (the pitting potential E_{pit}, the repassivation potential E_{rp}), thus providing standard environment for pitting corrosion evaluation. Inhibitor performance is based its capacity to anodically influence the pitting potential higher potential [22]. Thus this investigation aims to evaluate the pitting corrosion inhibition of 2-Amino-5-ethyl-1, 3, 4-thiadiazole on the electrochemical behaviour of austenitic stainless steel in dilute sulphu-

[1] The article is published in the original.

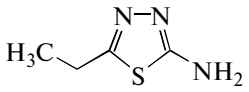

Fig. 1. Chemical structure of 2-amino-5-ethyl-1, 3, 4-thiadiazole (TTD).

ric acid, contaminated with recrystallised sodium chloride.

EXPERIMENTAL PROCEDURE

Material

Commercially available Type 304 austenitic stainless steel was used for all experiments of average nominal composition; 18.11% Cr, 8.32% Ni and 68.32% Fe. The material is cylindrical with a diameter of 18 mm.

Inhibitor

2-Amino-5-ethyl-1, 3, 4-thiadiazole (TTD) a colorless, solid flakes obtained directly from SMM Instrument, South Africa, is the inhibitor used. The structural formula of TTD is shown in Fig. 1. The molecular formula is $C_4 H_7 N_3 S$, while the molar mass is 129.18 g mol^{-1}.

TTD was prepared in concentrations of 0.125, 0.25, 0.375, 0.5, 0.625 and 0.75% respectively.

Test Media

3 M sulphuric acid with 3.5% recrystallised sodium chloride addition of Analar grade were used as the corrosion test media.

Preparation of Test Specimens

The cylindrical stainless steel (18 mm dia.) was mechanically cut into a number of test specimens of dimensions in length ranging from 17.8 and 18.8 mm coupons. The two surface ends of each specimen were ground with Silicon carbide abrasive papers of 80, 120, 220, 800 and 1000 grits. They were then polished with 6.0 μm to 1.0 μm diamond paste, washed with distilled water, rinsed with acetone, dried and stored in a dessicator for linear polarization test.

Linear Polarization Resistance

Linear polarization measurements were carried out using, a cylindrical coupon embedded in resin plastic mounts with exposed surface of 254 mm^2. The electrode was prepared with specific grades of silicon carbide paper, polished to 6 μm, rinsed by distilled water and dried with acetone. The studies were performed at ambient temperature with Autolab PGSTAT 30 ECO CHIMIE potentiostat and electrode cell containing 200 ml of electrolyte, with and without TTD. A graphite rod was used as the auxiliary electrode and silver chloride electrode (SCE) was used as the reference electrode. The steady state open circuit potential (OCP) was noted. The potentiodynamic studies were then made from −1.5 V *versus* OCP to +1.5 mV *versus* OCP at a scan rate of 0.00166 V/s. The corrosion current density (I_{corr}) and corrosion potential 'observed' (E_{corr}) were determined from the Tafel plots of potential *versus* log current. The corrosion rate (R), the degree of surface coverage (θ) and the percentage inhibition efficiency ($\%IE$) were calculated from equation (1) as follows

$$R = \frac{0.00327 \times I_{corr} \times \mathrm{Eq}}{D}. \quad (1)$$

Where I_{corr} is the current density in μA/cm^2, D is the density in g/cm^3; Eq is the specimen equivalent weight in grams;

The percentage inhibition efficiency ($\%IE$) was calculated from corrosion rate values using the equation (2).

$$\%IE = 1 - \left[\frac{R2}{R1}\right] \times 100, \quad (2)$$

where $R1$ and $R2$ are the corrosion rates in absence and presence of inhibitors, respectively.

Scanning Electron Microscopy Characterization

The surface morphology of the uninhibited and inhibited stainless steel specimens was investigated after the corresponding weight-loss analysis in 3 M H_2SO_4 solutions using Jeol scanning electron microscope for which SEM micrographs were recorded.

RESULTS AND DISCUSSION

Polarization Studies

Potentiostatic potential was cursorily examined −1.5 V to +1.5 V vs. Ag/AgCl at a scan rate of 0.00166 mV s^{-1} for equilibrium state analysis. The effect of the addition of TTD on the anodic and cathodic polarization curves of austenitic stainless steel (type 304) in 3 M H_2SO_4 solutions was studied at ambient temperature. Figure 2a–g shows the polarization curves of the stainless steel in absence and presence of TTD at specific concentrations in 3 M H_2SO_4 while Fig. 3 shows the relationship between inhibition efficiency ($\%\ IE$) and inhibitor concentration for TTD.

TTD adsorption on austenitic stainless steel is non-dependent on its percentage concentration in the acid solution due to the instantaneous electrochemical action and impact of the organic compound, obstructing the electrolytic diffusion of corrosive anions onto the steel at the concentrations studied. There was a significant decrease in corrosion rate in the acid solutions, but the electrochemical parameters varied differentially from 0% TTD concentration, indicating

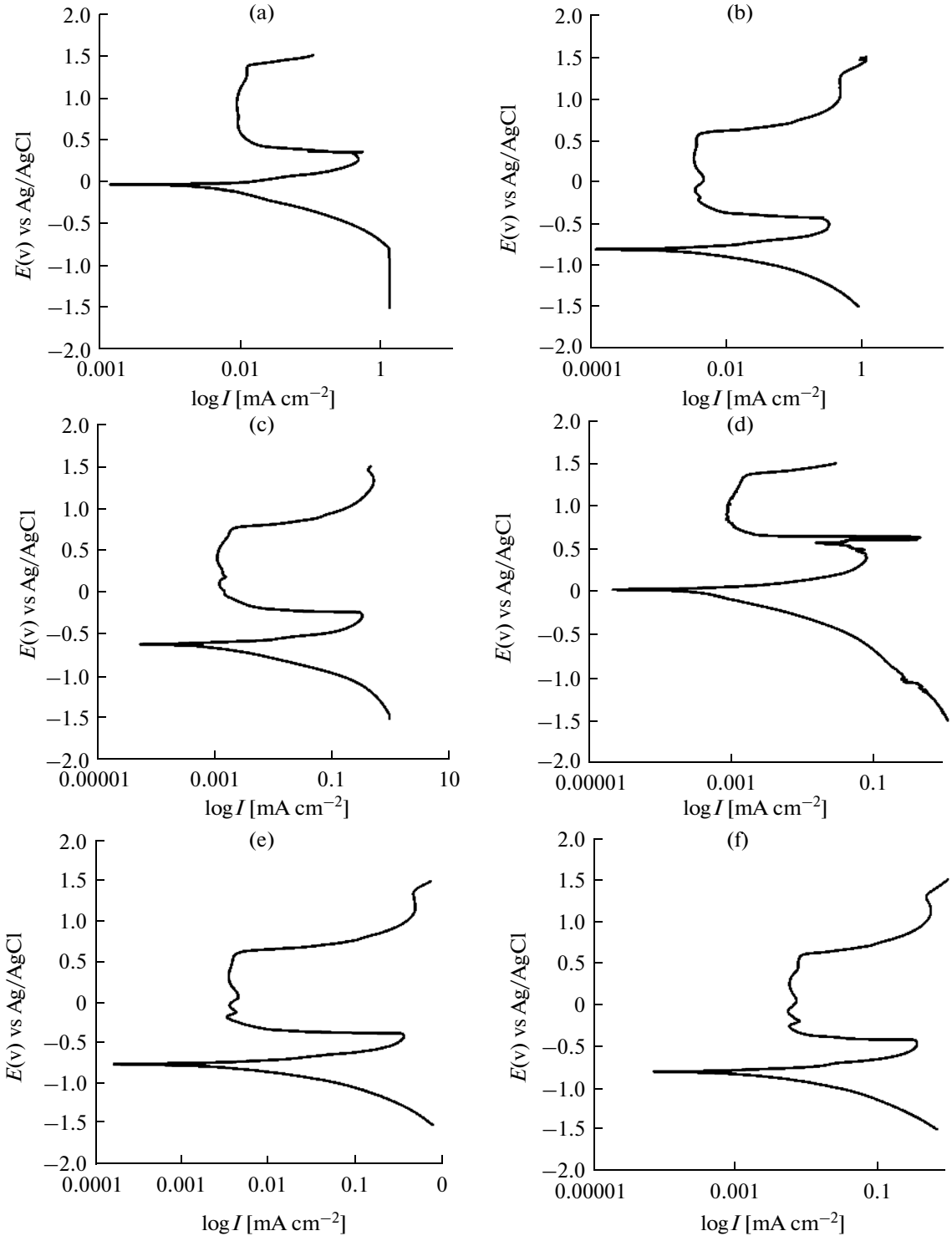

Fig. 2. (a–g) Polarization Curve of austenitic stainless steel (0–15% TTD) in 3 M H_2SO_4.

TTD influence on the electrochemical process responsible for corrosion degradation. Changes in the cathodic and anodic Tafel constants with TTD concentrations contrast the control concentration without TTD addition, signifying suppression of redox reactions responsible for corrosion reaction mechanism through the surface inhibiting effect of the compound. The electrochemical behaviour of TTD is based on adsorption and formation of a compact barrier film on the steel electrode surface. This is justified

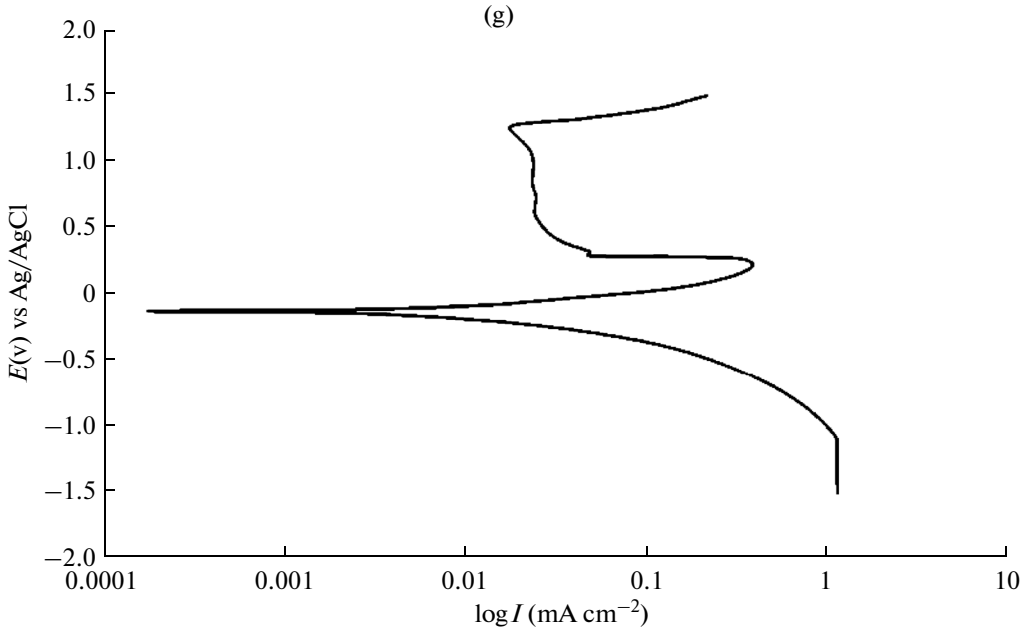

Fig. 2. (Contd.).

from the values of corrosion current and corrosion current density when compared to the values of the control concentration of 0% TTD.

Observation of Table 1 shows the displacement of the corrosion potential towards less noble potentials variably with increase in TTD concentration, thus passivation of iron. This is further confirmed from the corrosion rate values. The observation can also be attributed to electrolytic deposition of TTD cations on the stainless steel in the form of crystalline white precipitates due to interaction between the functional component of the inhibitor molecule and the steel surface. This effectively protects the steel surface against further electrochemical corrosion reactions. TTD showed cathodic inhibiting characteristics in the acid solution based on the corrosion potential displacement, an indication of its tendency to inhibit the cathodic reactions of the corrosion process.

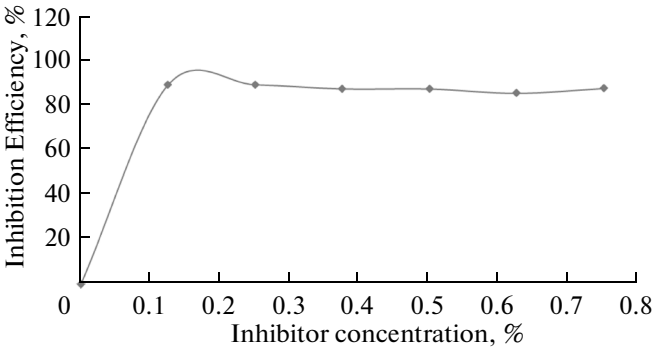

Fig. 3. Relationship between *%IE* and inhibitor concentration for polarization test in 3 M H_2SO_4.

The electrochemical variables such as, corrosion potential 'observed' (E_{corr}), corrosion current (i_{corr}), corrosion current density (I_{corr}), cathodic Tafel constant (*bc*), anodic Tafel constant (*ba*), surface coverage (θ), Pitting potential (E_{pit}) and percentage inhibition efficiency (*%IE*) were calculated and given in Table 1, while Nucleation resistance (NR), repassivation capacity (RC) corrosion potential 'calculated' (E_{corr}) and passivation range are shown in Table 2. The corrosion current density (I_{corr}) and corrosion potential 'observed' (E_{corr}) were determined by the intersection of the extrapolating anodic and cathodic Tafel lines. *%IE* was calculated from Eq. (3)

$$\%IE = \frac{R1 - R2}{R1}\%. \quad (3)$$

*R*1 and *R*2 are the corrosion current densities in absence and presence of TTD respectively.

The maximum displacement of E_{corr} values at –61 mV in the cathodic shows the inhibitor to be theoretically mixed but yet overwhelmingly a cathodic type from the E_{corr} values (Table 1). The mechanism of corrosion inhibition is most probably due to surface kinetic electrochemical process which inevitably results in diffusion control of the corrosive ions. In the acid solutions the values of anodic and cathodic Tafel constants of the control specimen (0%) differs greatly from specimens with TTD addition, thus TTD, influences redox electrochemical process despite its strong affinity for cathodic inhibition reactions. The corrosion current density is also changed with TTD addition.

Table 1. Data obtained from polarization resistance measurements for austenitic stainless steel in 3 M H_2SO_4 at specific concentrations of TTD

Sample	Inhibitor concentration, %	*ba*, V/dec	*bc*, V/dec	E_{corr}, 'Observed', V	I_{corr}, A/cm^2	i_{corr}, A	Corrosion Rate, mm/yr	R_p, Ω/cm^2	Inhibition Efficiency, %
A	0	0.364	0.242	0.343	9.35E-03	2.38E-02	9.602	1.61E+00	0
B	0.125	0.079	0.15	0.34	1.03E-03	2.62E-03	1.057	1.97E+00	88.99
C	0.25	0.029	0.074	0.326	1.03E-04	2.61E-04	1.053	3.52E+00	89.03
D	0.375	0.191	0.078	0.282	1.20E-04	3.05E-04	1.233	2.12E+00	87.16
E	0.5	0.157	0.113	0.332	1.20E-03	3.05E-03	1.233	2.52E+00	87.16
F	0.625	0.033	0.082	0.336	1.38E-04	3.51E-04	1.419	3.37E+00	85.22
G	0.75	0.089	0.091	0.332	1.18E-03	3.01E-03	1.214	1.17E+00	87.36

Table 2. Potentiostatic Values of Austenitic stainless steel in 3 M H_2SO_4/ TTD percentage concentrations

Sample	Inhibitor Concentration, %	Corrosion Potential, 'Calculated', E_{corr}	Potential, V	Repassivation Potential, V	Passivation Range, V	Nucleation Resistance, V	Repassivation Capacity, V
A	0	–0.036	1.278	0.511	0.767	1.314	0.547
B	0.125	–0.811	1.264	–0.372	1.636	2.075	0.439
C	0.25	–0.612	1.307	–0.177	1.484	1.919	0.435
D	0.375	0.014	1.322	0.561	0.879	1.367	0.488
E	0.5	–0.748	1.278	–0.319	1.597	2.026	0.429
F	0.625	–0.807	1.239	–0.367	1.606	2.046	0.44
G	0.75	–0.118	1.288	0.292	0.996	1.406	0.41

Pitting Corrosion Analysis of Austenitic Stainless Steel in 3 M H_2SO_4

The pit nucleation resistance NR ($E_{pit}-E_{corr}$), passivation range PR ($E_{pit}-E_{rep}$) and repassivation capacity RC ($E_{rep}-E_{corr}$) can be considered to be a measure of the susceptibility of alloys to pitting corrosion. Alloys exhibiting higher values of nucleation resistance and lower values of repassivation capacity are more resistant to pitting corrosion. The values of NR and RC are shown in Table 2. It is observed that the values of NC increased with increased in concentration of TTD, while the values of RC decreased proportionately. This proves that TTD increases the pitting corrosion resistance of the stainless steel in the harsh acidic solution. The corrosion inhibiting property of TTD to resist pitting corrosion is due to its influence on the electrochemical behaviour of the steel specimen and competitive reaction and adsorption onto the steel surface at the expense of corrosive anions (SO_4^{2-} and Cl^-).

Nucleation occurrence is due to the creation and evolution of metastable pits. These pit forms and develop for short period before repassivation, at potentials well beneath the pitting potential and during the induction time before the onset of stable pitting at potentials above the pitting potential. Nucleations symbolize the breakdown and repassivation of the passive film and occur extremely rapidly. Current increase depicts the initiation and progression of pits while the instantaneous decrease represents repassivation and pit termination. Specific accumulation of chloride complexes results in the formation of meta-soluble precipitate on the metal surface. This hampers the stability of the passive film at lower to higher potentials. The sequential hysteries in current value depict the sequential breakage and formation of occlusions during metastability which increases the porosity of the covering.

The presence chloride concentration excercebated the inhibiting action of TTD thus affects the values of

NR and CR respectively. This further confirms the impact of chlorides to the stainless steel because when the chloride content increases the capacity for the stainless steel to repassivate at lower potentials decreases. The difference between NR and CR for the polarization curves shows the passivation range on. The presence of a high concentration of adsorbed chloride ions at these sites will of course prevent further growth of the passive film and result in the establishment of active pits.

TTD wields strong influence on the potentiostatic behaviour of austenitic stainless steel in sulphuric acid as shown in the sharp contrast between Figs. 2a and 2b. The strong absorption characteristics of TTD delayed specimen failure after transpassivity due to second passivation, a phenomenon not observed before. This is due to the ability of TTD to delay the onset of corrosion by inhibiting the action of corrosive ions at high potential, thus inhibiting pit formation. It is understood that pit form due to the reactivity of chloride and sulphate ions in a redox process at potentials well below the threshold value. But with the addition of TTD at 0.125% a two stage passivation occurs. TTD formed strong covalent bonds through its functional groups and heteroatoms thus inhibiting the surface kinetics and diffusion responsible for corrosion.

It has been proven that TTD is a cathodic inhibitor in 3 M H_2SO_4 thus its adhesion to the steel surface is at specific cathodic sites sufficiently strong and stable at high potentials necessary to induce pitting. The second passivity phenomenon observed in Fig. 2b–2f is most probably due to TTD being able to reform its protective barrier/repassivate the steel slowing down the cathodic reaction or selectively precipitating on cathodic areas to increase the surface impedance and limit the diffusion of reducible species to these areas. This also in effect helps to prevent cathodic depolarization. The insoluble precipitate is responsible for the second passivity phenomenon. The process occurs at the transpassive region where stable pitting propagates but instead of complete specimen failure the material repassivates and sustains passivity until higher potentials at which critical pitting takes places as a results of electrolytic reactions that breaks down the covalent bonding between the metal surface and TTD.

The pitting potential values (E_{pit}), for austenitic stainless steel in 3 M H_2SO_4 + TTD percentage concentrations is shown in Table 2. The E_{pitt} value increased sharply with increasing TTD concentration from sample A (0% TTD), reaching its peak at 0.375% TTD before slightly declining to 0.75% TTD. Observation of these results shows the influence of TTD on the pitting corrosion resistance of metals samples. Addition of TTD significantly increased the potential at which pitting occurs, thus delaying pit formation. The repassivation potential and passivation range are also worth noting. With the exception of samples D and G (0.375% and 0.75% TTD), addition of TTD reduced the potential at which repassivation occurs i.e. the potential at which metastable pitting ceases and passivity restored. The passivation range, nucleation resistance and repassivation capacity values are parallel to the values of repassivation potential.

The results shows a material upon which TTD is capable of altering the electrochemical process of corrosion whereby the pitting potentials increased to more noble values and the repassivation potentials decreased to less noble values, these in effect increases the tendency of the material to nucleate and withstand pitting corrosion. At E_{pitt}, the initiation of pitting could be ascribed to the forced breakdown the covalent bonding between TTD and the metal surface. The precipitate formed cracks and there is a diffusion of SO_4^{2-}/Cl^- ions at some locations, thus penetrating it under high electric field across the film and accelerate localized anodic dissolution.

The SEM micrographs of the stainless steel specimen surfaces before and after immersion in the acid media with and without TTD are shown in Fig. 4a–4d, respectively. Figure 4a and 4b shows the steel sample before immersion, the lined surface with serrated edges is due to machining during sample preparation. Figure 4c shows the steel surfaces after 360 h of immersion in 3 M H_2SO_4 without TTD addition, while Fig. 4d shows the steel surface in the acid media with TTD addition. A rough porous surface is observed in Fig. 4c; macro and micro pits coupled with a badly corroded topography of the stainless steel surface are observable. This is due to destructive electrochemical reactions of chloride and sulphate ions resulting in the breakdown of the passive film of chromium oxide.

Figure 4c reveals a rough surface with large pits and cracks along the grain boundary at high magnification. The pit contains an unusual high content of sulphur and chloride atoms, proving them responsible for pit formation. The corrosion attack of the steel specimen is most probably a result of competitive adsorption/diffusion, whereby the anions move into the metal/liquid interface of the steel surface and displaces the species. They initiate and enhance the rate of iron diffusion into the solution. This is responsible for the uneven topography on the steel most especially at sites with flaws and inclusions. The corrosion is also observed to occur along the grain boundary due to its susceptibility to corrosion.

These pits are surrounded by iron oxide layer which almost fully covers the stainless steel surface, revealing that pit formation under these conditions occur continuously during the exposure period while iron oxide builds up over the surface. Most pits often grow with a porous cover which makes visual detection extremely difficult. The excess chromium occurs during active dissolution whereby chromium is enriched on the surface due to preferential dissolution of iron into the acid solution. Adsorption of the negatively charged anions causes an excess negative charge to build up on the steel surface leading to cations (protonated TTD

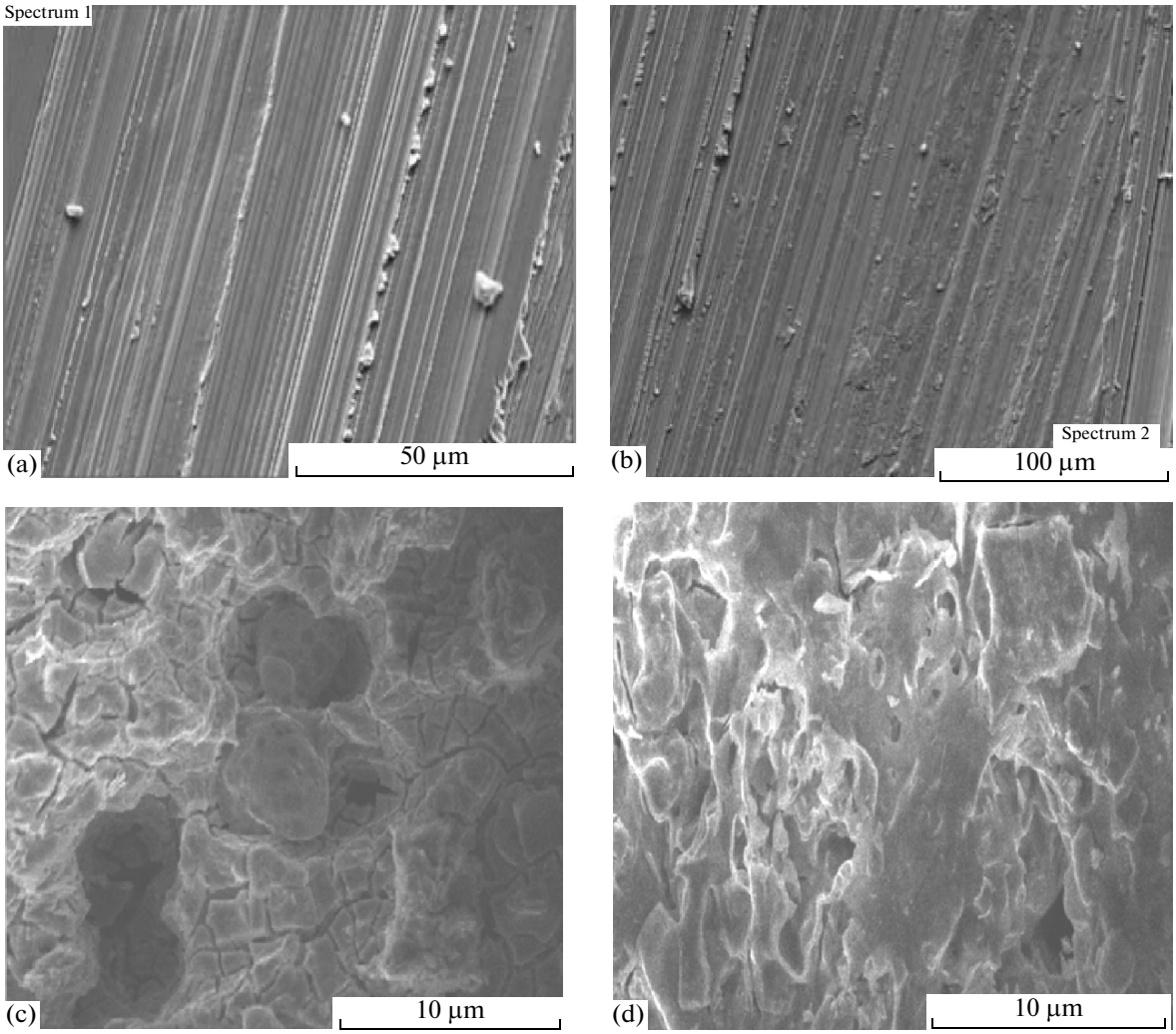

Fig. 4 SEM micrographs of: a—Austenitic stainless steel, b—Austenitic stainless steel, c—Austenitic stainless steel in 3 M H_2SO_4, d—Austenitic stainless steel in 3 M H_2SO_4 with TTD.

molecules) adsorption on the steel surface due to electrostatic attraction. This is responsible for the SEM image in Fig. 4d. The protective film is in the form of solid white crystalline precipitates which strongly adhered to the steel through chemisorption mechanism. These precipitates prevents diffusion of chlorides/sulphates and Fe^{2+}.

CONCLUSION

Potentiodynamic polarization tests on pitting corrosion behaviour of austenitic stainless steel (type 304) in dilute sulphuric acid with recrystallised sodium chloride addition in the presence of 2-amino-5-ethyl-1, 3, 4-thiadiazole inhibiting compound showed that the pitting corrosion potential (E_{pit}), of the steel increased significantly with increase in concentration of TTD. In the presence of the inhibiting compound the steel was far less vulnerable to pitting corrosion in comparison to results from the control sample without TTD addition. The pitting corrosion susceptibility significantly decreased proportionately with increase in concentration of TTD.

REFERENCES

1. Ramana, K.V.S., Anita, T.S., Mandal, S., et al., *Mater. Desalinization*, 2009, vol. 30, p. 3770.
2. Ramya, S., Anita, T. and Shaikh, H., *Corros. Sci.*, 2010, vol. 52, p. 2114.
3. Almarshad, A.I. and Jamal, D., *J. Appl. Electrochem.*, 2004, vol. 34, p. 67.
4. Nakayama, T. and Oshida, Y., *Corrosion*, 1968, vol. 24, p. 336.
5. Schweitzer, P.A., *Metallic Materials: Physical, Mechanical, and Corrosion Properties*, New York: Marcel Dekker, 2003, 1st ed.

6. Schweitzer, P.A., *Encyclopedia of Corrosion Technology*, New York: Marcel Dekker, 2004, 2nd ed.
7. Kudo, K.T., Shibata, G., Okamoto, G., and Sato, N., *Corros. Sci.*, 1968, vol. 8, p. 809.
8. Okamoto, G., *Corros. Sci.*, 1973, vol. 13, p. 471.
9. Galvele, J.R., *Corros. Sci.*, 1981, vol. 21, p. 551.
10. *Standard Guide G48-92, Annual Book of ASTM Standards*, 1994.
11. Ibrahim, M.A.S., Abd El Rehim, S.S. and Hamza, M.M., *Mater. Chem. Phys.*, 2009, vol. 115, p. 80.
12. Szklarska-Smialowska, Z., *Pitting Corrosion of Metals*, Houston, USA: Natl. Assoc. Corros. Eng., 1986.
13. Strehblow, H.H., in *Corrosion Mechanisms in Theory and Practice*, Marcus, P. and Oudar, J., Eds., New York, 1995.
14. Natishan, P.M., Kelly, R.G., Frankel, G.S., and Newman, R.C., *Electrochem. Soc., Proc.*, 1995, vol. 95, p. 15.
15. Frankel, G.S., *Mater. Sci. Forum*, 1997, vol. 247, p. 1.
16. Frankel, G.S., *J. Electrochem. Soc.*, 1998, vol. 145, p. 2186.
17. Maurice, V., Klein, L.H. and Marcus, P., *Electrochem. Solid-State Lett.*, 2001, vol. 4, p. B1.
18. Pawel, S.J., Stansbury, E.E and Lundin, C.D., *Corrosion*, 1989, vol. 45, no. 2, p. 125.
19. Baker, M.A. and Castle, J.E., *Corros. Sci.*, 1993, vol. 34, no. 2, p. 667.
20. Nogueira, T.M. C and Mattos, O.R., *Electrochem. Methods Corros. Res.,* 1986, vol. 8, p. 43.
21. Haupt, S. and Strehblow, H.H., *Corros. Sci.*, 1995, vol. 37, no. 1, p. 43.
22. Kaneko, M. and Issacs, H.S., *Corros. Sci.*, 2002, vol. 44, p. 1825.